Int J Clin Exp Med 2019;12(4):3272-3282
www.ijcem.com /ISSN:1940-5901/IJCEM0079447

Original Article

Therapeutic efficacy of *Xiaotan Sanjie* Formula on microsatellite instability of human gastric cancer MKN-45 cells and exploration of the underlying mechanism

Min Ye[1*], Li-Juan Xiu[1*], Tao Pang[2*], Ye Lu[1], Xuan Zhang[1], Jing-Yu Xu[1], Jian-Peng Jiao[1], Xuan Liu[1], Ying Zhao[1], Feng Wu[1], Bei Pei[1], Xiao-Qiang Yue[1], Pin-Kang Wei[1], Da-Zhi Sun[1]

Departments of [1]Traditional Chinese Medicine, [2]Pharmacy, Changzheng Hospital, Second Military Medical University, Shanghai, China. [*]Equal contributors and co-first authors.

Received February 1, 2017; Accepted October 5, 2018; Epub April 15, 2019; Published April 30, 2019

Abstract: Objective: To evaluate the therapeutic efficacy and explore the action mechanism of *Xiaotan Sanjie* Formula (*XSF*) on microsatellite instability (MSI) in human gastric cancer MKN-45 cells. Methods: The therapeutic efficacy of *XSF* on human gastric cancer MKN-45 cell proliferation was detected by CCK-8. Five MSI loci (D17S250, D2S123, D5S346, Bat-25 and Bat-26) were detected by STR Genotyping. The effect of *XSF* on the expression of MSI proteins of hMLH1, TGFβRII, IGFRII and Bax was analyzed by Western blot and RT-PCR. Results: *XSF* inhibited the proliferation of human gastric cancer MKN-45 cells in a time-dependent manner. When these MKN-45 cells were amplified to the five MSI loci, both D2S123 and D5S346 showed MSI with two peaks. After 48-h intervention with *XSF,* the mutation of D2S123 and D5S346 loci tended to be stabilized; the relative expression level of hMLH1, TGFβRII and Bax mRNA was increased in varying degrees, and the expression level of IGFRII mRNA tended to decrease, while the expression level of IGFRII protein was increased significantly ($P<0.05$). Conclusion: *XSF* inhibited MSI of human gastric cancer MKN-45 cells, probably by up-regulating MSI-associated hMLH1, TGFβRII, IGFRII and Bax gene and protein expressions, and IGFRII protein expression.

Keywords: Human gastric cancer MKN-45 cell, microsatellite instability, *Xiaotan Sanjie* Formula (XSF)

Introduction

The structure of cancer prevalence is undergoing changes. At present, the incidence and mortality of gastric cancer is next to lung cancer, ranking the second of solid tumors. In the world context, gastric cancer mainly occurs in China, Japan and South Korea. The number of gastric cancer detected yearly in China accounts for 42% of the total number worldwide, totaling 400,000 newly diagnosed cases each year, among which about 300,00 (75%) cases ended with death [1]. Therefore, it is an indispensable and urgent task to further explore the mechanism underlying the development and progression of gastric cancer so as to invent better intervention therapies on this devastating malignancy. More experimental studies have demonstrated that microsatellite instability (MSI) is closely associated with the development and progression of gastric cancer [2-4]. When MSI occurs, some specific genes such as TGFβRII, IGFRII and Bax may undergo frame-shift mutations at various loci of apoptosis signaling networks, thus preventing cell apoptosis from occurring and finally leading to uncontrolled tumor growth [5-7].

Based on years of clinical experience and practice, Professor Pin-Kang Wei from Changzheng Hospital (Shanghai, China) has developed a Chinese herbal *Xiaotan Sanjie* Formula (*XSF*), literally meaning a dispersing-phlegm-and-eliminating-stagnation preparation [8] and achieved satisfactory clinical outcomes, as represented by the significantly improved quality of life of patients with advanced gastric cancer [9]. *XSF* was approved as a traditional Chinese medi-

Table 1. The ingredients of *Xiaotan Sanjie* Formula (XSF) and corresponding percentages (accurate to 1 decimal place)

Chinese name	Latin name	Percentage
Ban-xia	Pinelliae rhizoma	12.7%
Nan-xing	Rhizoma arisaematis	12.7%
Fu-ling	Poria cocos	12.7%
Zhi-shi	Aurantii fructus immaturus	8.5%
Chen-pi	Citri reticulatae viride pericarpium	7.6%
Quan-xie	Scorpio	5.1%
Wu-gong	Scolopendra	7.6%
Ji-nei-jin	Galli gigerii endothelium corneum	12.7%
Bei-mu	Fritillariae cirrhosae bulbus	7.6%
Bai-jie-zi	Semen brassicae	7.6%
Gan-cao	Glycyrrhiza uralensis Fisch	5.1%

cine (TCM) patent drug in 2006 (China Patent No.: ZL200610029063.5). Some other experiments have also demonstrated that *XSF* can inhibit tumor recurrence and metastasis [10, 11]. The aim of the present study was to further explore the action mechanism of *XSF* on MSI in human gastric cancer via a drug serum in vitro experiment to observe and analyze MSI-associated up-regulation of hMLH1, TGFβRII, IGFRII and Bax gene and protein expressions, and IGFRII protein expression.

Materials and methods

Experimental materials

Human gastric cancer cell line MKN-45 was purchased from the Cell Resources of Shanghai Institutes for Life Sciences of the Chinese Academy of Sciences (Shanghai, China).

XSF used in this study was a granule dosage form (Batch No.: 130608) prepared by the Pharmaceutical Preparation Center of Changzheng Hospital and officially approved by China Drug and Food Administration (CFDA) for use within the Hospital. The main ingredients of *XSF* are listed in **Table 1**.

Tegafur (50 mg × 100 tablets; QILU Pharmaceutical Co., Ltd., Jinan, China; Batch No.: 206003LD) was used as the control.

Animal care and use

All rats used in this study were given the appropriateness of experimental procedures. They were lawfully acquired, and their retention and use in all cases were in compliance with the national and local laws and regulations, and the Institutional Animal Care and Use Committee (IACUC) of Shanghai Laboratory Animal Co., Ltd. (SLAC) Guide for Care and Use of Laboratory Animals. The minimal number of rats was used in the experiment. This study was specifically approved by IACUC (approval No.: SLAC-2015012-3002).

The rats received every consideration for their comfort, and were properly housed, fed and kept in a sanitary and specific-pathogen-free (SPF) grade laminar flow cabinet of a 12:12 light cycle with the illumination time automatically controlled from 8:00 AP to 20:00 PM in the animal house of Shanghai Experimental Animal Center of the Chinese Academy of Sciences (Shanghai, China).

The mobility, fur color, appetite and stool texture of the rats were monitored daily. During the period of drug administration, the rats were healthy and in a good physical condition with no sign of illness, unexpected death or other adverse events.

Animal grouping

Fifteen SD rats were equally randomized to three groups: a normal saline (NS) blank control group, a *XSF* group, and a Tegafur group.

Drug administration

Animals in *XSF* group received intragastric (i.g.) lavage of *XSF* at a concentration of 1.3 g/ml per rat (200 g), which was 10 times the daily standard dose (78 g) for a 60 Kg tumor-bearing adult patient, 1 ml at a time, bid.

Animals in Tegafur group received i.g. lavage of Tegafur at a concentration of 16.7 mg/ml for a rat (200 g), which was 10 times the daily dose (1000 mg) for a 60 Kg tumor-bearing adult patient, 1 ml at a time, bid.

Animals in NS group received the same volume of i.g. NS, bid.

Drug administration was continued for four days in all groups. At 8:00 AM of the fifth day, a

daily dose of the drug was administered at a time, and the animals were deprived of food with free access to water 12 h before the last lavage.

Blood sampling

On the fifth day, the rats were anesthetized with 4.5% chloral hydrate aldehyde (0.001 ml/kg) 1 h after i.g. lavage, and 3-5 ml whole blood was drawn from each animal via the posterior orbital venous plexus. Then, the animals were euthanized with a lethal dose of 4.5% chloral hydrate aldehyde (0.003 ml/kg) and not used in any other experiments.

Drug serum preparation

The whole blood samples were tranquilized for 3-4 h, centrifuged at 3000 rpm for 10 min to collect the serum, and then centrifuged again at 5000 rpm to collect the serum for the second time. After activating the complement by water bath at 56°C for 30 min and being filtrated through a 0.22 μm filter, the blood samples were prepared into a blank drug serum (containing 10% blank drug serum+5% FBS+85% RPMI1640); a *XSF* serum (containing 10% *XSF* serum+5% FBS+85% RPMI1640); and a Tegafur serum (containing 10% Tegafur serum +5% FBS +85% RPMI1640) as designed, and then stored at -80°C.

Human gastric cancer cell line MKN-45 grouping

Cells were devided into three groups: XSF serum intervention group (XSF group), Tegafur serum intervention group (Tegafur group), and normal saline serum intervention group (NS group).

Transmission electron microscopy (TEM) sample preparation

MKN-45 cells intervened with the designated drugs for 48 h were collected by using a 1.5 ml taper bottom centrifuge tube. After centrifugation and removal of the medium, cells were rinsed with phosphate buffer (PB) and fixed in 4% paraformaldehyde and heavy density medium at 4°C for 4 h. The frozen cell sap was cut into three 1 mm^3 pieces, rinsed thoroughly, and fixed with osmic acid for 2 h, washed with PB, added in sequence with 30%, 50%, 70% and 90% ethanol and 90% acetone for 10 min, and 100% acetone for 10 min × 3, embedded, polymerized, sliced into ultra-thin sections, stained, and observed under a TEM.

Cell proliferation

The cell suspension was seeded to 96-well plates at a concentration of 5 × 10^4/ml (100 μl/well), grouped, administered with the designated drugs, and cultured at 37°C and 5% CO_2 for 72 h. After replacing the medium with 100 μl fresh medium and adding 10 μl CCK-8, cells were cultured for 3 h, and optical density (OD) was detected at 450 nm by using a microplate reader for three times. The inhibitory rate (%) = 1 - [(experiment well OD - blank well OD)/(control well OD - blank well OD)] × 100%.

Cell scratch test

MKN-45 cells were adjusted to 1 × 10^5/ml per well and seeded to 6-well plates. After cells became confluent all over the plate, they were adjusted to a density of 100% convergence and washed with PBS twice. After washing out the drifting cells, they were administered with the designated drugs and cultured at 37°C and 5% CO_2 overnight for cell starvation. After 24-h starvation, cells were scratched with a sterile 20 μl Tip, washed with PBS twice to remove the drifting cells, and photographed under an inverted microscope (× 20) at 0, 12 and 24 h. The results of photography were measured to observe the healing ability of the scratch as an indicator of the cell migration ability.

Cell invasion

MKN-45 cells were digested, suspended in serum-free medium, counted, and then seeded into the Transwell chambers. After drug administration, the Transwell chambers were placed in 24-well plates, cultured for 24 h, washed with PBS to remove cells in the chambers, fixed, and stained with crystal violet. The Transwell membranes were cut off, placed on the slides, observed by microscopy, photographed by randomly selecting 6 places, and counted.

Detection of MSI-associated proteins (hMLH1, TGFβRII, IGFRII and Bax) by Western blot

After cell lysis, protein concentrations were determined according to the manufacturer's instructions (NanJing KeyGen Biotech, item No.: KGPBCA). The small amount (40 μg) of the

Table 2. RT-PCR primer sequences

Site	Primer No.	Primer sequence	Length
D17S250	D17S250.F	GGAAGAATCAAATAGACAAT	151 bp
	D17S250.R	GCTGGCCATATATATATTTA	
D2S123	D2S123.F	AAACAGGATGCCTGCCTTTA	211 bp
	D2S123.R	GGACTTTCCACCTATGGGAC	
D5S346	D5S346.F	GGTTGTTTCCGTAGTATATGG	295 bp
	D5S346.R	TTGGGAAAGAAGACTAAATCA	
Bat-25	Bat-25.F	TCGCCTCCAAGAATGTAAGT	126 bp
	Bat-25.R	ATTCTGCATTTTAACTATGGCTCT	
Bat-26	Bat-26.F	TCACTGTCTGCGGTAATCAAG	400 bp
	Bat-26.R	TAGAGTGGGCTGAGATTGTGC	

protein sample was electrophoresed by 10% SDS-PAGE and transferred to the PVDF membrane, sealed with 5% skimmed milk at room temperature for 2 h, primary antibody of GAPDH (1:5000, Shanghai Kangcheng Biotech, item No.: KC-5g5), and hMLH1, TGFβRII, IGFRII and Bax (1:1000, Cell Signaling Technology, item No.: 3515P, 11888S, 9759P, 2772S), incubated at 4°C overnight, washed with TBST three times, added with HRP-labeled goat anti mouse secondary antibody (1:2000, Southern biotech, item No.: 4052-05), incubated at room temperature for 1 h, washed with TBST three times, added with ECL substrate, imaged and photographed in the WB gel imaging system.

Detection of MSI-associated proteins (hMLH1, TGFβRII, IGFRII and Bax) by RT-PCR

Total RNA was extracted by using a total RNA extract kit. The purity and concentration of the total RNA were detected with an ultraviolet spectrophotometer to determine the reverse cDNA sample volume. Total RNA was reverse transcribed into cDNA using a cDNA reverse transcription kit. PCR primers were designed with PRIMER 5.0 software in reference with the related literature. Mix, cDNA and the primers were added into RT-PCR 96-well plates under the amplification conditions of 95°C 5 min, 95°C 10 s, 60°C 30 s, totaling 40 cycles. The relative expression level was calculated by 2^(-ΔΔCT).

STR genotyping analysis

Chromosomes were extracted according to the instruction of the extraction kit. The PCR primers were designed and amplified according to the five microsatellite DNA fragments (D2S123, D3S1067, D3S1577, D17S250 and Bat-26) recommended by the American National Cancer Institute (NCI) [12, 13]. All primer sequences were cited from NCBI uniSTS database. The primers were synthesized by Shanghai Bright Handsome Biotechnologies Co., Ltd. (Shanghai, China). The PCR products were purified and directly sent for capillary electrophoresis on the 3130 sequenator after addition of the interior label. Data were collected and treated automatically by Data Collection Software to produce the raw sample file under the conditions of pre-degeneration at 95°C for 5 min, degeneration at 95°C for 1 min, annealing for 1 min (D17S250, D2S123, D5 S346, Bat-25 56°C, Bat-26 54°C), extension at 72°C for 30 s, totaling 30 cycles, and finally extension at 72°C for 1 min. The primers are listed in **Table 2**.

Judgment criteria

The five microsatellite loci were detected by PCR according to the criteria of Boland et al [12]. Positive MSI was classified as the following three conditions: instability of two or more than two loci as high microsatellite instability (MSI-H); instability of one locus as low microsatellite instability (MSI-L); and no-locus instability as microsatellite stable (MSS). MSI occurrence (%) = the number of samples with gene displacement/the total number of samples × 100%.

Statistical methods

All analyses were performed with SPSS13.0 Statistical Software. All dose data were shown by mean ± SD ($\bar{x}\pm s$). Data of normal distribution were tested by homogeneity of variance test with Levene, and analyzed by single factor analysis of variance; data of small samples were analyzed by nonparametric Kruskal-Wallis H test, and pairwise comparison was analyzed by Mann-Whitney U test. Values of $P<0.05$ were considered statistically significant.

Results

TEM results

Cells were collected for TEM observation after 48-h intervention of human gastric cancer MKN-45 cells in different groups. As shown in

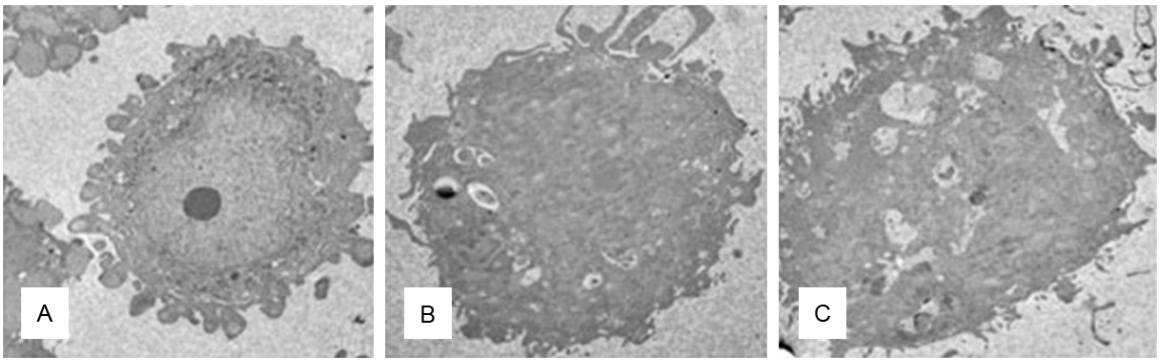

Figure 1. Ultra-structure of human gastric cancer MKN-45 cells. A. NS group 1 × 1500. B. *XSF* group 1 × 1500. C. Tegafur group 1 × 1500. NS = normal saline. A: The tumor cell capsule in NS group was intact, and the morphology of the nucleus, mitochondrion and endoplasmic reticulum was generally normal. B: In *XSF* group, the cytomembrane of tumor cells was not continuous; the nucleus was pyknotic; the chromosome heterochromatin was congested; the mitochondrial structure was damaged with the crest disappearing; the endoplasmic reticulum was expanded; vacuoles were seen in the cytoplasm; cells were in an apoptotic state. C: In Tegafur group, huge vacuoles were seen in the cytoplasm; the nucleus was pyknotic; the mitochondrial structure disappeared; and the endoplasmic reticulum was expanded.

Table 3. Effects of the drugs in different groups on the proliferation of human gastric cancer MKN-45 cells

Group (*n*=6)	OD (0 h)	OD (12 h)	OD (24 h)	OD (48 h)	*P*
Normal saline	0.156±0.015	0.281±0.020	0.484±0.050	0.862±0.115	0.00
XSF	0.155±0.015	0.236±0.023	0.503±0.066	0.731±0.047*	
Tegafur	0.155±0.021	0.247±0.025	0.454±0.041	0.535±0.076*,△	

*$P<0.05$, *vs.* NS group; △$P<0.05$, *vs. XSF* group.

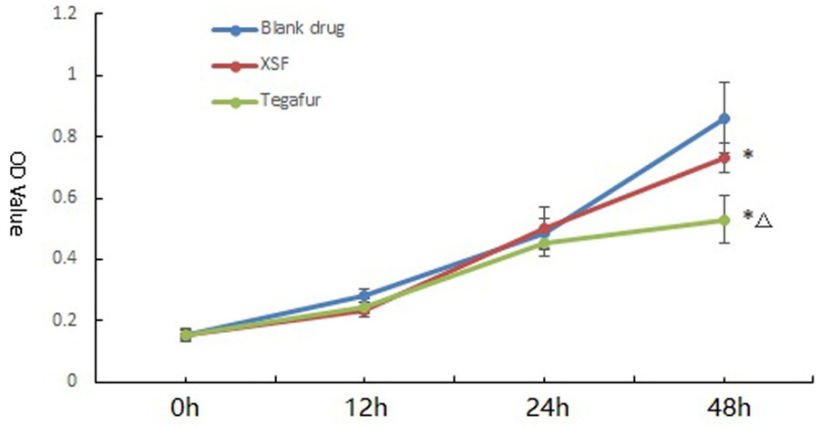

Figure 2. Growth curves of intervention with different drugs on human gastric cancer MKN-45 cells. *P<0.05, vs. NS group; △P<0.05, vs. XSF group.

Figure 1, the tumor cell capsule in NS group was intact, and the morphology of the nucleus, mitochondrion and endoplasmic reticulum was generally normal; in *XSF* group, the cytomembrane of the tumor cells was not continuous; the nucleus was pyknotic; the chromosome heterochromatin was congested; the mitochondrial structure was damaged with the crest disappearing; the endoplasmic reticulum was expanded; vacuoles were seen in the cytoplasm; and cells were in an apoptotic state; and in Tegafur group, huge vacuoles were seen in the cytoplasm; the nucleus was pyknotic; the mitochondrial structure disappeared; and the endoplasmic reticulum was expanded. The results demonstrated that *XSF* could destruct the cytoarchitecture of MKN-45 cells.

Cell proliferation

As shown in **Table 3**, there was no significant difference in OD between the three groups at 0 h ($P>0.05$). One-way ANOVA showed significant differences in OD between the three groups at 48 h ($P=0.000$). Further paired comparison showed significant differences in OD between *XSF* and NS groups ($P=0.022$), between Tegafur and NS groups ($P=0.000$), and between *XSF* and Tegafur groups ($P=0.001$). Growth curves showed an inhibitory effect of *XSF* on the proliferation of human gastric cancer MKN-45 cells in a time-dependent manner (**Figure 2**).

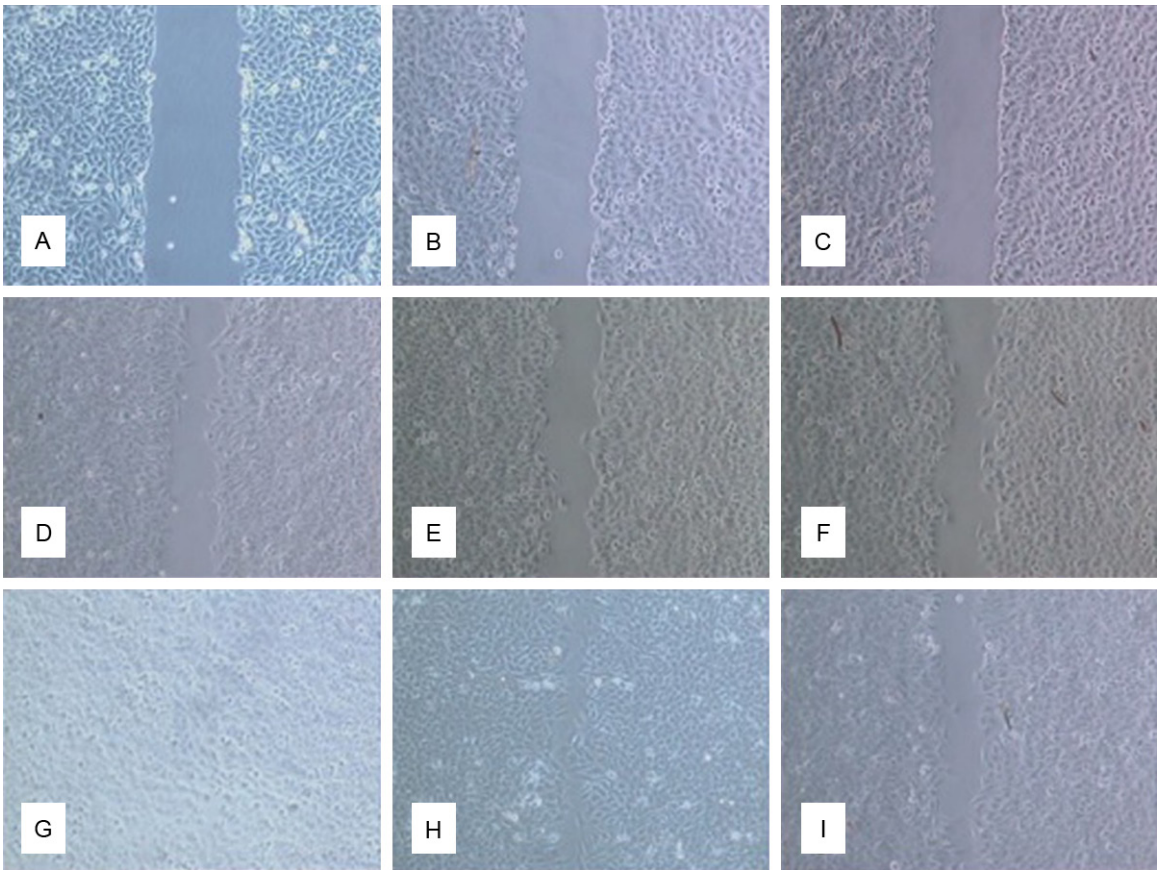

Figure 3. Effects of different drugs on the migration ability of human gastric cancer MKN-45 cells. A. NS group (0 h), the initial scratch wound. B. *XSF* group (0 h), the initial scratch wound. C. Tegafur group (0 h), the initial scratch wound. D. NS group (12 h), cell healing 12 h after scratching. E. *XSF* group (12 h), cell healing 12 h after scratching. F. Tegafur group (12 h), cell healing 12 h after scratching. G. NS group (24 h), cell healing 24 h after scratching. H. *XSF* group (24 h), cell healing 24 h after scratching. I. Tegafur group (24 h), cell healing 24 h after scratching. NS = normal saline. Almost all cell scratches healed at 24 h in NS group, while the cell scratches in *XSF* and Tegafur groups remained unhealed. Compared with MKN-45 cells in *XSF* group, MKN-45 cells in Tegafur group migrated more slowly within 24 h.

Table 4. The number of MKN-45 cells penetrating the matrix membrane in different groups

Group (*n*=6)	24 h	48 h
Normal saline	15.67±2.08	22.33±2.08
XSF	11.67±0.58*	22.00±1.00
Tegafur	12.67±1.53	16.33±2.89*,△
P value	0.043	0.023

*$P<0.05$, *vs.* NS group; △$P<0.05$, *vs. XSF* group.

Repair of cell scratch

After 24-h starvation of human gastric cancer MKN-45 cells seeded in the 6-well plate, cells were scratched with a sterile 20 μl Tip along the plate bottom in the form of a transverse straight line, and photographed at 0, 12 and 24 h after scratching to compare the migration ability of the cells. As all cell scratches healed after 24 h, no further experiment was performed in subsequent hours. As shown in **Figure 3**, almost all cell scratches healed at 24 h in NS group, while the cell scratches in *XSF* and Tegafur groups remained unhealed. Compared with MKN-45 cells in *XSF* group, MKN-45 cells in Tegafur group migrated more slowly within 24 h, suggesting that both *XSF* and Tegafur exerted an inhibitory effect on the migration of MKN-45 cells, and this effect was stronger in Tegafur group as compared with that in *XSF* group.

Cell invasion ability

The result of one-way ANOVA showed that there were significant differences in the ability of MKN-45 cells in penetrating the Matrigel matrix membrane between the three group at 24 h ($P=0.043$). Further paired comparison showed

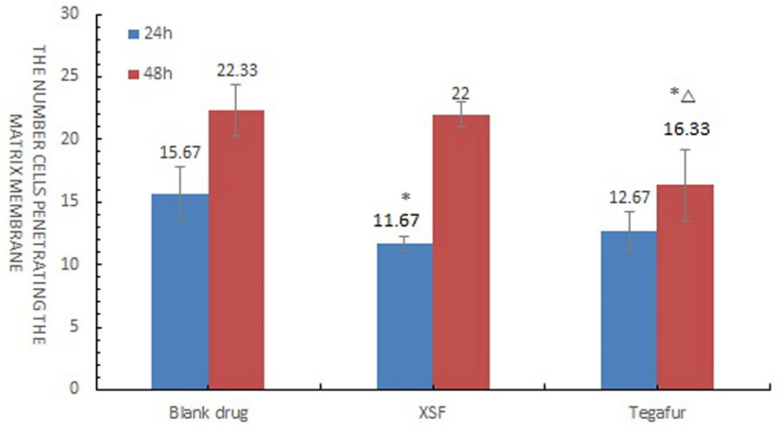

Figure 4. The number of MKN-45 cells penetrating the matrix membrane in different groups. $^{*}P<0.05$, *vs.* NS group; $^{\triangle}P<0.05$, *vs. XSF* group.

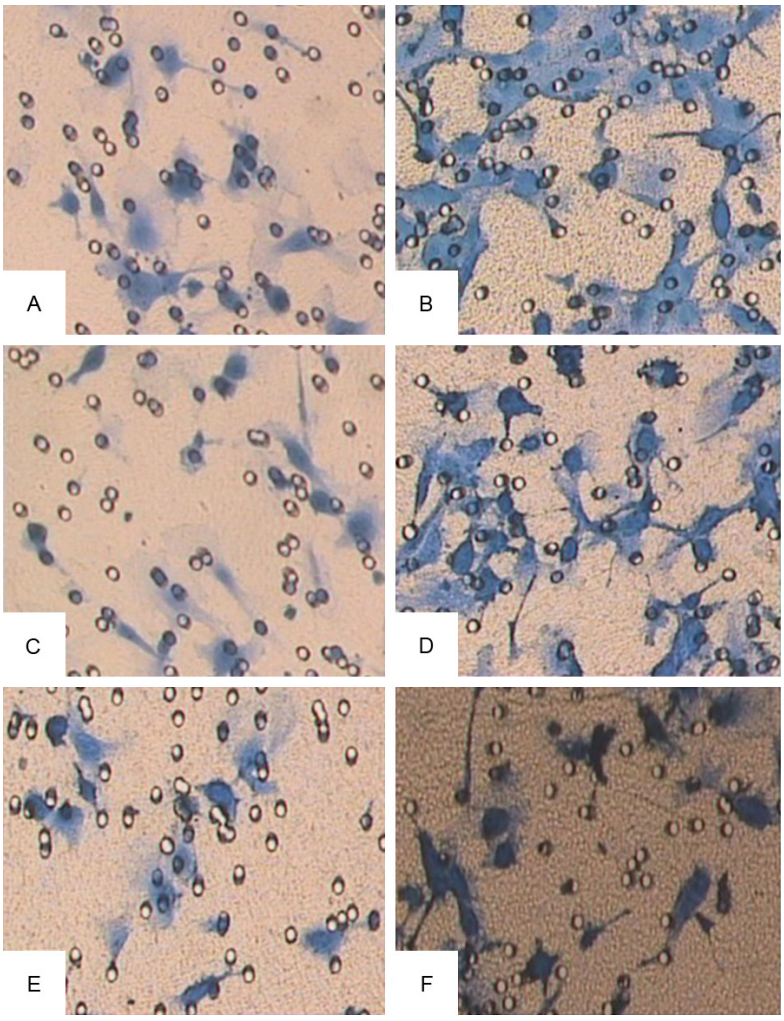

Figure 5. Effects of different drugs on invasiveness of human gastric cancer MKN-45 cells (× 400). A. NS group (24 h), MKN-45 cells penetrating the matrix at 24 h. B. NS group (48 h), MKN-45 cells penetrating the matrix at 48 h. C. *XSF* group (24 h), MKN-45 cells penetrating the matrix at 24 h. D. *XSF* group (48 h), MKN-45 cells penetrating the matrix at 24 h. E. Tegafur group (24 h), MKN-45 cells penetrating the matrix at 24 h. F. Tegafur group (48 h), MKN-45 cells penetrating the matrix at 48 h. NS = normal saline. At 24 h, the number of MKN-45 cells penetrating the Matrigel matrix membrane in *XSF* group was significantly smaller than that in NS group (P=0.018). The number of MKN-45 cells penetrating the Matrigel matrix membrane in Tegafur group was also decreased. The number of MKN-45 cells penetrating the Matrigel matrix membrane in NS group was increased after 48 h, while the number of MKN-45 cells penetrating the Matrigel matrix membrane both in XSF group and in Tegafur group was decreased after 48 h.

that the number of MKN-45 cells penetrating the Matrigel matrix membrane in *XSF* group was significantly smaller than that in NS group (P=0.018). The number of MKN-45 cells penetrating the Matrigel matrix membrane in Tegafur group was also decreased, but there was no significant difference (P>0.05) between NS and Tegafur groups. One-way ANOVA still showed statistical differences between the three groups at 48 h (P=0.023). Further paired comparison showed a significant difference between NS and Tegafur groups (P= 0.014). The number of MKN-45 cells penetrating the Matrigel matrix membrane in *XSF* group was also decreased, but there was no significant difference (P>0.05) between NS and *XSF* groups. There was significant difference between *XSF* and Tegafur groups at 48 h (P=0.017) (**Table 4**). These results suggest that both XSF and Tegafur could reduce the invasive ability of MKN-45 cells (**Figure 4**). These effects were most pronounced at 24 h for XSF, and at 48 h for Tegafur (**Figure 5**).

Table 5. Comparison of the size, height and area of D17S250, D2S123, D5 S346, Bat-25 and Bat-26 between different groups

Group	n	Item	Bat-25	Bat-26	D2S123		D5S346		D17S250
			Peak 1	Peak 1	Peak 1	Peak 2	Peak 1	Peak 2	Peak 1
Normal saline	10	Size (bp)	124.11	394.77	206.28	210.27	284.77	286.81	146.45
		P-height (RFU)	3618±627	611.31±298	1768±634	1831±454	1463±392	2116±607	4881±1857
		P-area (RFU·S)	28111±5352	30639.26±16291	37651±13879	20303±5800	17212±4563	24795±6741	75619±40472
Tegafur	10	Size (bp)	122.96	394.52	—	209.81	285.5	—	146.97
		P-height (RFU)	1353±585	221±92	—	846±312	534±193	—	2095±731
		P-area (RFU·S)	9647±4138	8228±3293	—	9724±3914	5696±1798	—	15175±5436
XSF	10	Size (bp)	125.17	394.43	—	209.7	285.63	—	146.92
		P-height (RFU)	1499±638	183±50	—	956±131	263±81	—	2326±219
		P-area (RFU·S)	10724±4785	7487±2048	—	11365±1911	3117±1177	—	17323±1425

Table 6. Grayscale analysis of the expressions of MSI-associated proteins after intervention with different drugs

Group (n=3)	hMLH1	TGFβRII	IGFRII	Bax
Normal saline	0.612±0.062	0.359±0.043	0.222±0.031	0.242±0.009
XSF	0.897±0.111*	0.825±0.143△	1.732±0.251△	1.368±0.234△
Tegafur	0.880±0.097*	0.969±0.077△	2.342±0.636△	1.114±0.138△

*P<0.05 *vs.* NS group; △P<0.01 *vs.* NS group.

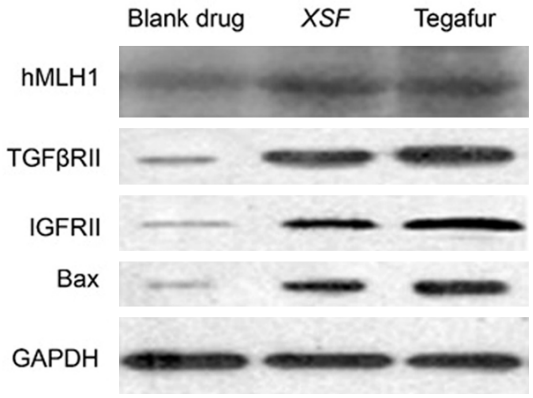

Figure 6. Change in the expression of MSI-associated proteins after intervention with different drugs. *P<0.05, *vs.* NS group, △P<0.01, *vs.* NS group.

MSI occurrence in different groups and comparison of the size, height and area of the five loci between different groups

Of the five loci (D17S250, D2S123, D5 S346, Bat-25 and Bat-26), MSI with two peaks was 100% (10/10) at D5S346 (including 70% MSI-H and 30% MSI-L) and 70% (7/10) at D2S123. In both *XSF* and Tegafur groups, Peak 1 at D2S123 and Peak 2 at D5S346 disappeared and the corresponding loci showed MSS (**Table 5**). These results indicate that both *XSF* and Tegafur could regulate MSI at the loci of D2S123 and D5S346, and the target locus and effect were the same. The above-mentioned results indicate that *XSF* could inhibit the MSI of MKN-45 cells.

Changes in MSI-associated proteins of hMLH1, TGFβRII, IGFRII and Bax in vitro

One-way ANOVA showed significant differences in the gray diagram and gray value of the four proteins between the three groups. Further paired analysis showed that the expression levels of the four proteins were significantly increased in *XSF* and Tegafur groups as compared with those in NS group, while there was no significant difference between *XSF* and Tegafur groups, suggesting that *XSF* could increase the protein expression of hMLH1, TGFβRII, IGFRII and Bax (**Table 6**; **Figure 6**).

Detection of MSI-associated mRNAs by RT-PCR in vitro

Inter-group comparison showed that the relative expression level of hMLH1 was increased (P=0.027<0.05) in XSF and Tegafur groups. The further pairwise comparisons found that the expression level of hMLH1 was statistically significant (P=0.033<0.05) in the comparison between Tegafur and NS groups; while there was no statistically significant in the comparison between XSF and NS groups, but they were the same as the results of WB, i.e. there was a tendency of increasing its expression level. Regarding the expressions of TGFβRII and Bax groups, there was no statistically significant in the inter-group comparison (P>0.05), the XSF

Table 7. Relative expression level of MSI-associated mRNA in human gastric cancer MKN-45 cells

Group (n=3)	Normal saline	*XSF*	Tegafur	P
hMLH1	17.70±0.80	23.63±2.05	40.27±4.32*	0.027
TGFβRII	6.17±0.77	6.64±0.97	9.13±2.12	0.079
IGFRII	13.73±1.34	8.01±0.57	7.94±0.64	0.066
Bax	0.72±0.13	0.80±0.03	2.36±0.30	0.051

*P<0.05 vs. NS group.

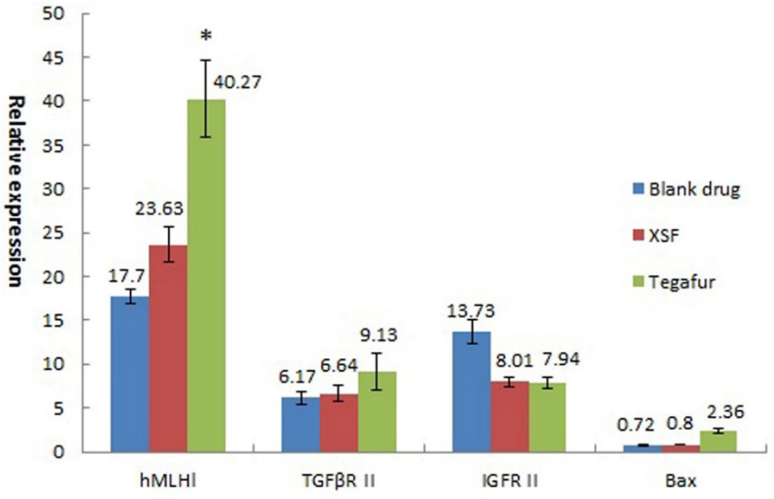

Figure 7. Relative expression level of MSI-associated mRNA by RT-PCR. *P<0.05, *vs.* NS group.

and Tegafur groups, however, showed the tendency of increasing their expression levels (**Table 7**; **Figure 7**).

Discussion

With the more profound understanding about malignant tumors, increased numbers of clinical and experimental studies in recent years have demonstrated that other than activation of oncogenes and inactivation of anti-oncogenes, MSI is a new mechanism in the initiation of malignant tumors. Since the discovery of MSI in hereditary non-polyposis colorectal cancer (HNPCC) in 1993 [14], MSI has been detected in multiple cancers, including gastric cancer [15, 16], breast cancer [17], ovarian cancer [18], lung cancer [19] and cholangiocarcinoma [20]. The occurrence of MSI in gastric cancer is about 14-45% [21-23], or even high as 76% [24, 25].

Although large numbers of studies have demonstrated the presence of the MSI phenomenon in solid tumors, the mechanism underlying the effect of MSI in the development and progression of gastric cancer remains elusive. Since the discovery of mismatched repair (MMR) enzymes by Holliday et al in 1964 [26], many subsequent studies have demonstrated the universal existence of the MMR system in *E. coli* and higher eukaryotes. The MMR system has been shown to play important roles in DNA replication, repair and recombination. Altogether, nine genes have been identifying to participate in the MMR system. MMR genes are composed of a series of DNA base-mismatched enzyme molecules that have specific repair functions to repair mismatched and paired DNA bases, thus safeguarding genomic stability and DNA replication fidelity. When loss of the expression of a particular mismatched gene occurs, the error occurring during the replication process cannot be repaired, resulting in the increase or decrease in DNA gene fragments, known as MSI, which is closely associated with the development and progression of gastric cancer [27]. Of the nine MMR genes, hMLH1 is reported to play a key role in the occurrence of MSI [28]. Some studies [29] showed that the expression of hMLH1 was positively correlated with MMR in colon cancer. Change in MMR may affect corresponding target genes such as TGFβRII, IGFRII and Bax. At the same time, these genes can regulate cell growth, proliferation and apoptosis. Mutation of these genes is called the second mutational event of MSI tumors [30]. Functional change of these genes would further affect the development and progression of gastric cancer, and eventually affect the therapeutic effect [31].

XSF is modified from *ErchenTang Decoction,* a classical TCM formula for cough due to phlegm caused by dysfunction of the spleen, and has been used in clinical practice for more than 40 years in China for preventing tumor recurrence

and metastasis, especially gastric cancer [8, 10, 11], and improving the quality of life of patients with gastric cancer [9]. These pharmacological effects of *XSF* have also been studied and confirmed in animal experiments and clinical trials for more than 20 years at the biomolecular level [32, 33].

It was fund in the present study that *XSF* had a remarkable inhibitory effect on the proliferation of human gastric cancer MKN-45 cells in a time-dependent manner. In addition, *XSF* could also ameliorate MSI of human gastric cancer MKN-45 cells (D2S123 and D5S346), and stabilize the unstable microsatellite loci, most probably by increasing the expression of mismatched protein hMLH1 and second-locus mutation protein TGFβRII, IGFRII and Bax. The inconsistent expression of IGFRII at the mRNA and protein levels may result from the increased amount of protein in the process of protein modification, thus decreasing protein degradation and prolonging the half-life of the proteins. This postulation needs to be further verified in our ongoing study. At any rate, this study provides a new idea and approach on studying the mechanism of *XSF* intervention on gastric cancer.

Acknowledgements

This work was supported by grants from the National Natural Science Foundation of China (No.: 81273910).

Disclosure of conflict of interest

None.

Address correspondence to: Da-Zhi Sun, Xiao-Qiang Yue and Pin-Kang Wei, Department of Traditional Chinese Medicine of Changzheng Hospital Affiliated to The Second Military Medical University, #415 Fengyang Road, Shanghai 200003, China. Tel: +86-21-81885473; Fax: (021) 63520020; E-mail: sundz@smmu.edu.cn (DZS); yuexiaoqiang@163.com (XQY); weipinkang@126.com (PKW)

References

[1] Chen W, Zheng R, Baade PD, Zhang S, Zeng H, Bray F, Jemal A, Yu XQ and He J. Cancer statistics in China, 2015. CA Cancer J Clin 2016; 66: 115-132.

[2] Kim YB, Lee SY, Kim JH, Sung IK, Park HS, Shim CS and Han HS. Microsatellite instability of gastric and colorectal cancers as a predictor of synchronous gastric or colorectal neoplasms. Gut Liver 2016; 10: 220-227.

[3] Velho S, Fernandes MS, Leite M, Figueiredo C and Seruca R. Causes and consequences of microsatellite instability in gastric carcinogenesis. World J Gastroenterol 2014; 20: 16433-16442.

[4] Zhu L, Li Z, Wang Y, Zhang C, Liu Y and Qu X. Microsatellite instability and survival in gastric cancer: a systematic review and meta-analysis. Mol Clin Oncol 2015; 3: 699-705.

[5] Iacopetta BJ, Soong R, House AK and Hamelin R. Gastric carcinomas with microsatellite instability: clinical features and mutations to the TGF-beta type II receptor, IGFII receptor, and BAX genes. J Pathol 1999; 187: 428-432.

[6] Nogueira AM, Carneiro F, Seruca R, Cirnes L, Veiga I, Machado JC and Sobrinho-Simoes M. Microsatellite instability in hyperplastic and adenomatous polyps of the stomach. Cancer 1999; 86: 1649-1656.

[7] Yamamoto H, Imai K and Perucho M. Gastrointestinal cancer of the microsatellite mutator phenotype pathway. J Gastroenterol 2002; 37: 153-163.

[8] Wei P, Xu L, Sun D, Shi J, Qin Z and Lu Y. Relations between phlegm and generation and development of gastric cancer. J Tradit Chin Med 2008; 28: 152-155.

[9] Sun DZ, Jiao JP, Zhang X, Xu JY, Ye M, Xiu LJ, Zhao Y, Lu Y, Liu X, Zhao J, Shi J, Qin ZF and Wei PK. Therapeutic effect of Jinlongshe Granule () on quality of life of stage IV gastric cancer patients using EORTC QLQ-C30: a double-blind placebo-controlled clinical trial. Chin J Integr Med 2015; 21: 579-586.

[10] Sun DZ, Ju DW, He J, Lu Y, Wu F, Li C and Wei PK. Tumor interstitial fluid and postoperative recurrence of tumors: an experimental study for verifying hypothesis of "tumor-phlegm microenvironment". Chin J Integr Med 2010; 16: 435-441.

[11] Sun DZ, Jiao JP, Ju DW, Ye M, Zhang X, Xu JY, Lu Y, He J, Wei PK and Yang MH. Tumor interstitial fluid and gastric cancer metastasis: an experimental study to verify the hypothesis of "tumor-phlegm microenvironment". Chin J Integr Med 2012; 18: 350-358.

[12] Boland CR, Thibodeau SN, Hamilton SR, Sidransky D, Eshleman JR, Burt RW, Meltzer SJ, Rodriguez-Bigas MA, Fodde R, Ranzani GN and Srivastava S. A national cancer institute workshop on microsatellite instability for cancer detection and familial predisposition: development of international criteria for the determination of microsatellite instability in colorectal cancer. Cancer Res 1998; 58: 5248-5257.

[13] Perucho M. Correspondence re: C.R. Boland et al., A National Cancer Institute workshop on

microsatellite instability for cancer detection and familial predisposition: development of international criteria for the determination of microsatellite instability in colorectal cancer. Cancer Res 1998; 58: 5248-5257. Cancer Res 1999; 59: 249-256.

[14] Aaltonen LA, Peltomaki P, Leach FS, Sistonen P, Pylkkanen L, Mecklin JP, Jarvinen H, Powell SM, Jen J, Hamilton SR, et al. Clues to the pathogenesis of familial colorectal cancer. Science 1993; 260: 812-816.

[15] Falchetti M, Saieva C, Lupi R, Masala G, Rizzolo P, Zanna I, Ceccarelli K, Sera F, Mariani-Costantini R, Nesi G, Palli D and Ottini L. Gastric cancer with high-level microsatellite instability: target gene mutations, clinicopathologic features, and long-term survival. Hum Pathol 2008; 39: 925-932.

[16] Zhao Y, Zheng ZC, Luo YH, Piao HZ, Zheng GL, Shi JY, Zhang T and Zhang JJ. Low-frequency microsatellite instability in genomic di-nucleotide sequences correlates with lymphatic invasion and poor prognosis in gastric cancer. Cell Biochem Biophys 2015; 71: 235-241.

[17] Smolarz B, Makowska M, Samulak D, Michalska MM and Romanowicz H. Gly322Asp and Asn127Ser single nucleotide polymorphisms (SNPs) of hMSH2 mismatch repair gene and the risk of triple-negative breast cancer in Polish women. Fam Cancer 2015; 14: 81-88.

[18] Lee JH, Cragun D, Thompson Z, Coppola D, Nicosia SV, Akbari M, Zhang S, McLaughlin J, Narod S, Schildkraut J, Sellers TA and Pal T. Association between IHC and MSI testing to identify mismatch repair-deficient patients with ovarian cancer. Genet Test Mol Biomarkers 2014; 18: 229-235.

[19] Shen C, Wang X, Tian L and Che G. Microsatellite alteration in multiple primary lung cancer. J Thorac Dis 2014; 6: 1499-1505.

[20] Moy AP, Shahid M, Ferrone CR, Borger DR, Zhu AX, Ting D and Deshpande V. Microsatellite instability in gallbladder carcinoma. Virchows Arch 2015; 466: 393-402.

[21] Kim KM, Kwon MS, Hong SJ, Min KO, Seo EJ, Lee KY, Choi SW and Rhyu MG. Genetic classification of intestinal-type and diffuse-type gastric cancers based on chromosomal loss and microsatellite instability. Virchows Arch 2003; 443: 491-500.

[22] Mizoshita T, Tsukamoto T, Cao X, Otsuka T, Ito S, Takahashi E, Nakamura S, Nakamura T, Yamamura Y and Tatematsu M. Microsatellite instability is linked to loss of hMLH1 expression in advanced gastric cancers: lack of a relationship with the histological type and phenotype. Gastric Cancer 2005; 8: 164-172.

[23] Wu M, Semba S, Oue N, Ikehara N, Yasui W and Yokozaki H. BRAF/K-ras mutation, microsatellite instability, and promoter hypermethylation of hMLH1/MGMT in human gastric carcinomas. Gastric Cancer 2004; 7: 246-253.

[24] Fleisher AS, Esteller M, Tamura G, Rashid A, Stine OC, Yin J, Zou TT, Abraham JM, Kong D, Nishizuka S, James SP, Wilson KT, Herman JG and Meltzer SJ. Hypermethylation of the hMLH1 gene promoter is associated with microsatellite instability in early human gastric neoplasia. Oncogene 2001; 20: 329-335.

[25] Leung WK, Kim JJ, Kim JG, Graham DY and Sepulveda AR. Microsatellite instability in gastric intestinal metaplasia in patients with and without gastric cancer. Am J Pathol 2000; 156: 537-543.

[26] Bronner CE, Baker SM, Morrison PT, Warren G, Smith LG, Lescoe MK, Kane M, Earabino C, Lipford J, Lindblom A, et al. Mutation in the DNA mismatch repair gene homologue hMLH1 is associated with hereditary non-polyposis colon cancer. Nature 1994; 368: 258-261.

[27] Hamelin R, Chalastanis A, Colas C, El Bchiri J, Mercier D, Schreurs AS, Simon V, Svrcek M, Zaanan A, Borie C, Buhard O, Capel E, Zouali H, Praz F, Muleris M, Flejou JF and Duval A. Clinical and molecular consequences of microsatellite instability in human cancers. Bull Cancer 2008; 95: 121-132.

[28] Shigeyasu K, Nagasaka T, Mori Y, Yokomichi N, Kawai T, Fuji T, Kimura K, Umeda Y, Kagawa S, Goel A and Fujiwara T. Clinical significance of MLH1 methylation and CpG island methylator phenotype as prognostic markers in patients with gastric cancer. PLoS One 2015; 10: e0130409.

[29] Martinez-Uruena N, Macias L, Perez-Cabornero L, Infante M, Lastra E, Cruz JJ, Miner C, Gonzalez R and Duran M. Incidence of -93 MLH1 promoter polymorphism in familial and sporadic colorectal cancer. Colorectal Dis 2013; 15: e118-123.

[30] Goel A, Arnold CN, Niedzwiecki D, Carethers JM, Dowell JM, Wasserman L, Compton C, Mayer RJ, Bertagnolli MM and Boland CR. Frequent inactivation of PTEN by promoter hypermethylation in microsatellite instability-high sporadic colorectal cancers. Cancer Res 2004; 64: 3014-3021.

[31] Yamamoto H and Imai K. Microsatellite instability: an update. Arch Toxicol 2015; 89: 899-921.

[32] Li CJ, Wei PK and Yue BL. Study on the mechanism of xiaotan sanjie recipe for inhibiting proliferation of gastric cancer cells. J Tradit Chin Med 2010; 30: 249-253.

[33] Shi J and Wei PK. Xiaotan Sanjie decoction inhibits interleukin-8-induced metastatic potency in gastric cancer. World J Gastroenterol 2015; 21: 1479-1487.